Thermodynamic analysis of secondary refrigeration loops: effects of slurry type and flow conditions

Michel Pons[a], Hong-Minh Hoang[b], Anthony Delahaye[b] and Laurence Fournaison[b]

[a] LIMSI-CNRS, Rue J. von Neumann, Campus, 91405 Orsay Cedex, FRANCE. michel.pons@limsi.fr (CA)
[b] IRSTEA, GPAN-Enerfri, 1 rue Pierre Gilles de Gennes CS10030, 92761 Antony Cedex, FRANCE.
hong-minh.hoang@irstea.fr ; Anthony.delahaye@irstea.fr ; laurence.fournaison@irstea.fr.

Abstract:

The refrigeration industry must face more and more restrictive regulations about the volume of refrigerant contained in the units. Those regulations aim to reduce the leaks of refrigerant toward the atmosphere, a serious hazard with respect to global warming potential. In the many cases when one central cooling unit distributes cold between several cold heat-exchangers with a long refrigerant circuit, inserting a secondary refrigeration loop, filled with a fluid most often neutral with respect to the environment, between the evaporator and the distributed heat-exchangers is a good way to reduce the refrigerant volume. When the secondary refrigerant is a two-phase fluid, namely a slurry, large enthalpy changes can be achieved over reduced temperature glides. Ice slurries have indeed been used for long in industrial environment. New classes of slurries are currently under study: the clathrate-hydrates. These ice-like crystalline compounds mainly made of water molecules arranged around host molecules, attract attention because their fusion temperatures lie over zero Celsius and can be adjusted to the application.

A numerical model of a two-phase secondary refrigeration loop was built-up for addressing the basic issues and all the energy transports and conversion processes involved from final use (herein air conditioning) to heat release to the atmosphere. Global analysis involves total energy consumption altogether with flow constraints in terms of turbulence (for avoiding crystal sedimentation) or pressure drops (not too high), so that each simulation is self-consistent. Exergy analysis of the whole process is also developed. Performance of various slurries, ranging from glycol-water mixture to clathrate-hydrate of CO_2+TBPB, are compared, first in terms of global performance, second in terms of irreversibility: that analysis evidences which parameters have the most influence on design and results, and how.

Keywords:
Hydrate, Refrigeration, Energy Efficiency, Second Law, Exergy.

1. Introduction

While cold production is a basic need in fields as various as food preservation, chemistry, electronics, transportation, or air-conditioning, it unfortunately accounts for 15% of the total electricity consumed in industrialized countries, and for 8% of their total emission of greenhouse gases. This emission is mainly due to leaks of refrigerant from the circuits, and current hydrofluorocarbon refrigerants have a high global warming potential. This is why regulation on refrigerants is more and more restrictive, especially in order to reduce leakage by limiting the amount of refrigerant contained in cooling units. There exist however many cooling units that distribute cold (under the form of condensed refrigerant) to several heat-exchangers which are spatially separated by tens of meters if not hundreds (*e.g.* in hospitals, supermarkets). In such cases, *secondary refrigeration* offers the opportunity to distribute the same amount of cold to the same users but from a central cooling unit limited in volume and with a fluid that can be safe to the environment [1]. Secondary refrigeration transports cold, either as sensible heat, *e.g.* chilled water, or as latent heat with phase change materials. Among the various two-phase fluids, suspensions of ice-crystals in an aqueous solution, called *slurries*, take advantage of the significant fusion enthalpy of ice, 333.6 kJ/kg [2]. Beyond academic studies, for instance on

the thermal properties of ice slurries [3-5], their application in industrial processes [6-8] shows that ice slurry has become a mature technology.

However, ice slurries cannot be used above 0°C, a temperature range with many usages of refrigeration. Hydrates or clathrates form a new and wide class of ice-like materials, currently under intense study, either of their thermodynamic equilibrium [9-11], their thermophysical properties [12,13], their kinetics [14,15], their equations of state [16,17], or advanced aspects of their application [18,19]. From the point of view of refrigeration, those phase-change materials have a twofold advantage: their enthalpy of fusion is rather close to that of ice (220-300 kJ/kg), and their melting temperature can easily be adapted to the desired level. Indeed, there exist many host molecules that, once combined with water, can form hydrates; each of those liquid-solid systems has a specific phase diagram and therefore specific melting point(s). In addition, two (and more) of those molecules, for instance one of them being gaseous, may be combined, thus forming so-called *mixed hydrates*, the melting point of which then depends on the gas pressure. Among those mixed hydrates, that of CO_2 + TBPB (tetra-n-butyl phosphonium bromide) raises special interest [20].

Compared to ice slurries, such new hydrates bring new features with respect to secondary refrigeration or cold storage. Those new features are related to their phase diagram, their rheology, and also to the fact that they now involve a gaseous phase. As long as secondary refrigeration was limited to ice slurries, thermodynamic analysis of such systems mainly consisted of reporting their performance [8,21-25]. Now that many alternative solutions exist, the thermodynamic analysis extends to optimization [26], comparison with other fluids [18], test and modelling [27], development of innovative concepts [28], or effects of the slurry production mode [29]. There are very few Second Law analyses, and they focus on the storage process [24,30] or on the pipe flow [31]. The present study aims to establish a global framework for thermodynamic analyses of secondary refrigeration.

2. Methodology and description of the model

2.1 Methodology

This study develops a first-order approach of secondary refrigeration in order to highlight the most important parameters with respect to thermodynamic efficiency through comparison of various slurries, ranging from the well-known slurry of ice crystals in water-glycol solution to the innovative one of mixed hydrate CO_2 + TBPB in TBPB solution. For that purpose, the refrigeration loop is reduced to its very essential components, and assumed to be operated in steady-state.

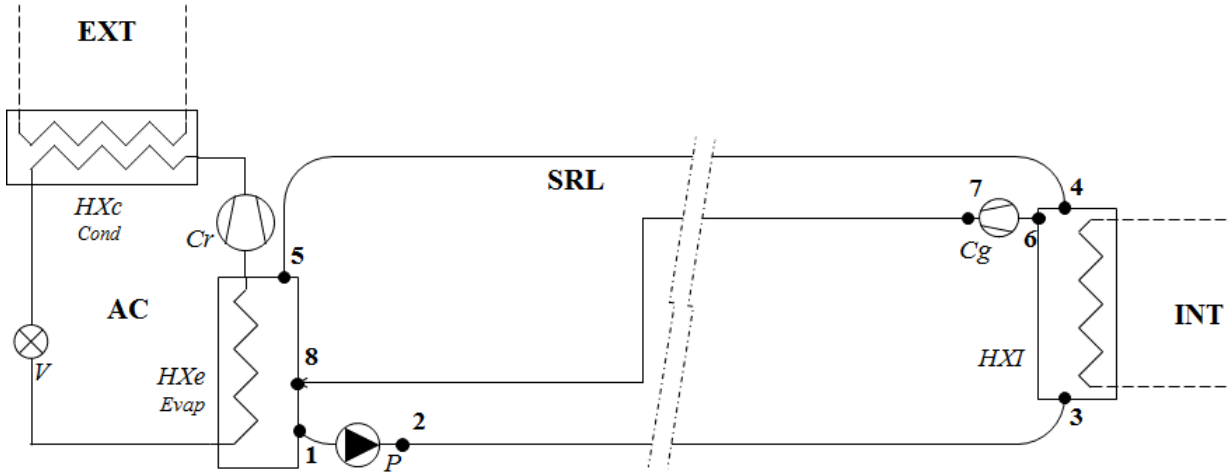

Fig. 1. Schematic of configuration investigated herein. The secondary refrigeration SRL loop (123451) transports heat from the air-conditioned internal space INT to the central air-conditioning unit AC, which rejects heat to the external air EXT. The refrigerant of the AC unit evaporates in the

heat-exchanger HXe, is compressed by the compressor Cr, condenses in HXc, and expands in the valve V. The pump P circulates the slurry in the SRL loop. If melting in HXI ever releases gas, this gas is re-pressurized (in the compressor Cg) in order to feed crystallization in HXe (line 678).

The analysis, First Law and Second Law, relies on numerical results obtained from a model of the configuration presented in Fig. 1. The present approach consists of prescribing:

- the rate of heat extraction at the heat-exchanger *HXI* $\dot{Q}_I$ (30kW)
- the temperatures T_I and T_E of the INT space and of the external air EXT (25°C and 40°C),
- the heat-transfer resistances R_I, R_e, and R_c of the three heat-exchangers HXI, HXe, and HXc (resp. 0.33, 0.33 and 0.29K/kW),
- the internal exergetic efficiency of AC cycle, η_{Bi}, that accounts for the various internal irreversibilities such as the isentropic efficiency of the compressor, the pressure drops, the effects of superheat or subcooling, etc.; the value η_{Bi}=0.8 is indeed smaller than usual values of compressor isentropic efficiencies,
- and of course the distance L between the heat exchanger HXI and the AC unit (50m).

Those figures are rather consistent with the experimental data of [8]. Then, for each of the slurries under study, a whole range of flow conditions in the SRL loop is scanned, from (large-diameter & low-velocity) to (small-diameter & high-velocity). Using thermodynamic relations and phenomenological formulae, the conditions of the slurry flow (velocity, Reynolds number and therefore intensity of turbulence, and total pressure drop) are evaluated, leading to a favoured configuration for which the flow is altogether, sufficiently turbulent (in order to avoid deposition of crystal particles along the circuit), with limited pressure drop (in order to prevent the circuit to be too strongly pressurised), and with limited pumping power (so that the corresponding energy consumption remains auxiliary with respect to that of the AC unit). Once the favoured configuration is designed for a given slurry, the First Law and Second Law analyses are developed, especially focusing on the total consumption of mechanical energy $\dot{W}_{tt}$ and the most important exergy losses.

2.2 Thermodynamic of the system

2.2.1. Slurry, crystal and gas

The description of the hydrate slurry relies on two companion assumptions. First, the minimal solid fraction of crystals in the slurry, X_4, at the outlet of HXI, is fixed at a non-zero value, namely 0.02. Indeed, when residual crystals are still present in the slurry in the heat exchanger HXe, they act as nucleation seeds that strongly accelerate the crystallization process. As a result, it can also be assumed that crystallization kinetics is fast enough for the solution-hydrate system to be close to its equilibrium as given by the phase diagram.

When the system variance is one (*e.g.* for CO_2-hydrate in pure water), the melting point is given by the gas pressure, which is herein assumed to be uniform along the SRL loop. Then, as the system always lies on the crystallization plateau, enthalpy of the slurry is straightforwardly related to the solid fraction X of the slurry: $\mathrm{d}h = -\Delta H \cdot \mathrm{d}X$.

When the system variance is two (*e.g.* for ice in mono-propylene-glycol solution, or CO_2+TBPB hydrate in water+TBPB solution), then the composition of the solution (solute fraction x, with a prescribed value for the fully melted solution, x_0) depends on X and on the composition of the crystals as defined by Y_w and Y_g. The relation is: $x = \left[x_0 \cdot (1 - X \cdot Y_g) - X \cdot (1 - Y_w - Y_g) \right] \Big/ \left[1 - X \right]$.

For pure ice, one obviously has Y_w=1 and Y_g=0. Moreover, the melting point now also depends on x, and on the gas pressure P when relevant, according to a function $T_m(x,P)$ given by the phase diagram.

As a consequence, a change in the solid fraction X always occurs with a temperature change, so that, when assuming uniform gas pressure, the enthalpy change is now:

$$\mathrm{d}h = \left\{ -\Delta H + \left[X \cdot c_{p,cr} + (1-X) \cdot c_{p,ls} \right] \cdot \left(\frac{\partial T_m}{\partial x} \right)_P \cdot \frac{\mathrm{d}x}{\mathrm{d}X} \right\} \cdot \mathrm{d}X \tag{1}$$

Lastly, the state reference can be chosen in such a way that the enthalpy and entropy of the gaseous phase in state 6 vanishes, so that the First Law balances (mass and energy conservation) yield:

$$\dot{m}_6 = \dot{m}_{s3} - \dot{m}_{s4} = Y_g \cdot (\dot{m}_{s3} \cdot X_3 - \dot{m}_{s4} \cdot X_4) \tag{2}$$

$$\dot{m}_{s4} \cdot h_4 - \dot{m}_{s3} \cdot h_3 = \dot{Q}_I \tag{3}$$

Once the solid fraction at point 3, X_3, is given, these equations yield the mass flow-rates $\dot{m}_{s3}$, $\dot{m}_{s4}$, and $\dot{m}_{s6}$. Using the density of the slurry, $\rho_s = \left[(1-X)/\rho_{ls} + X/\rho_{cr} \right]^{-1}$, the volume flow-rates are easily deduced. The next step consists of calculating the pressure drops in the circuit.

2.2.2. Flow conditions

The viscosity of non-Newtonian fluids, like slurries, mainly depends on the solid volume fraction $\phi = X \cdot \rho_s / \rho_{cr}$ and on the viscosity of the liquid phase. Once the diameter D of one circuit portion is given, the slurry velocity [$u = 4\dot{m}_s / (\rho_s \pi D^2)$] leads to the Reynolds number [$Re = \rho_s u D / \mu_s$] from which the friction factor f is evaluated by the Blasius relation. The pressure drop in that circuit portion is then deduced as: $\Delta P = f \cdot \rho_s \cdot u^2 \cdot (L + \Delta L_{HX}) / (2 \cdot D)$, where the pipe length L is complemented by the extra length ΔL_{HX} that phenomenologically accounts for the pressure drops in the heat exchangers HXI and HXe. Adding the different pressure drops along the slurry SRL loop yields the total pressure drop ΔP_{tt}, and the mechanical power of the pump P: $\dot{W}_P = \dot{m}_s \Delta P_{tt} / \rho_s$.

Applying the same approach for the gas line 6-8, while assuming a gas velocity of 2m/s and an overpressure of 25kPa for re-injecting the gas into HXe for crystallization, leads to the mechanical consumption of the compressor Cg, $\dot{W}_{Cg}$. As $\dot{W}_{Cg}$ occurs to be very small compared to $\dot{W}_P$ (less than 1% by far), it is not worth introducing the efficiency of the compressor Cg, the value of which has no influence at all on the results.

2.2.3. AC unit and total energy consumption

Energy conservation in the SRL loop leads to (4), while heat transfer in the heat-exchanger HXe (when neglecting the vapour superheat) yields the evaporation temperature (5):

$$\dot{Q}_e = \dot{Q}_I + \dot{W}_P + \dot{W}_{Cg} \tag{4}$$

$$T_e = T_4 - R_e \cdot \dot{Q}_e \tag{5}$$

Similar equations can be written for the heat-exchanger HXc and the condensation temperature:

$$\dot{Q}_c = \dot{Q}_e + \dot{W}_{Cr} \tag{6}$$

$$T_c = T_E + R_c \cdot \dot{Q}_c \tag{7}$$

Actually, the equations (5) and (7) are slightly approximated. First, the evaporated refrigerant may be superheated, say by 5K. For the R134A, such a superheat would represent only 2.5% of the latent heat of evaporation. Second, taking into account the temperature increase of the external air when it extracts the condensation heat (it surely does not remain at T_E) would require more details on the heat-exchanger, which is out of scope of the present study. Third, the resistances R_c and R_e are

independent of the mass flow rates. Reducing the crudeness of this assumption would require a refined description of all the components, which is beyond the scope of the present study.

The evaporation and condensation temperatures yield the *COP* of the endoreversible refrigeration cycle, from which the effective COP of the AC cycle is easily deduced as:

$$COP_{AC} = \frac{\dot{Q}_e}{\dot{W}_{Cr}} = \eta_{Bi} \cdot \frac{T_e}{T_c - T_e} \tag{8}$$

This set of non-linear equations is solved iteratively with the help of a Matlab in-house code, leading to the total energy consumption of the secondary refrigeration process: $\dot{W}_{tt} = \dot{W}_{Cr} + \dot{W}_P + \dot{W}_{Cg}$.

2.2.4. Exergy analysis

Whatever the variance of the hydrate-solution equilibrium, the entropy and exergy changes of the system are respectively $\mathrm{d}s = \mathrm{d}h / T_m$ and $\mathrm{d}b = \mathrm{d}h \cdot (1 - T_E / T_m)$. Then, the entropic mean temperature is defined as $T_m = \Delta h / \Delta s$ [32], where Δh and Δs are the total enthalpy and entropy changes occurring between the states 3 and 4 (5 and 1 by symmetry). The exergy analysis leads straightforwardly to the exergy losses of the process. The temperatures considered for the heat-exchanges [(9), (11), (13)] are, either uniform (heat-sources at T_E and T_I, refrigerant phase-changes at T_e and T_c), or the entropic mean temperature T_m. The mechanical energy of the pump P and compressor Cg is assumed (with a negligible loss of accuracy but a great gain of simplicity) to be dissipated toward a fluid at T_m (10), and then transported as heat toward the external air. The exergy loss in the AC unit can be written in various ways in function of $\dot{W}_{Cr}$ and $\dot{Q}_e$, the most convenient one is that given in (12).

$$\Delta\dot{B}_I = \dot{Q}_I \cdot T_E \cdot \left(T_m^{-1} - T_I^{-1} \right) \tag{9}$$

$$\Delta\dot{B}_P = \dot{W}_P \cdot T_E / T_m \;;\; \Delta\dot{B}_{Cg} = \dot{W}_{Cg} \cdot T_E / T_m \tag{10}$$

$$\Delta\dot{B}_e = \dot{Q}_e \cdot T_E \cdot \left(T_e^{-1} - T_m^{-1} \right) \tag{11}$$

$$\Delta\dot{B}_{AC} = \dot{W}_{Cr} \cdot T_E / T_c + \dot{Q}_e \cdot T_E \cdot \left(T_c^{-1} - T_e^{-1} \right) \tag{12}$$

$$\Delta\dot{B}_c = \dot{Q}_c \cdot T_E \cdot \left(T_E^{-1} - T_c^{-1} \right) \tag{13}$$

The flux of exergy produced by the process, $-\dot{Q}_I \cdot \left(1 - T_E / T_I\right)$, is the same for every slurry. When summing up the six exergy losses given in (9)-(13), where $\dot{Q}_e$ is to be replaced by $\dot{Q}_I + \dot{W}_P + \dot{W}_{Cg}$ and $\dot{Q}_c$ by $\dot{Q}_I + \dot{W}_P + \dot{W}_{Cg} + \dot{W}_{Cr}$, simple algebra leads to the global exergy balance (14), which confirms that the analysis is correct (the exergy input equals the produced exergy plus all the losses).

$$\dot{W}_{Cr} + \dot{W}_P + \dot{W}_{Cg} = -\dot{Q}_I \cdot \left(1 - T_E / T_I\right) + \sum_j \Delta\dot{B}_j \text{ , where } j \in \{I, P, Cg, e, AC, c\} \tag{14}$$

3. Results and discussion

3.1. Slurries under study and their thermophysical properties

The approach described in Section 2 is applied to various slurries, selected in such a way that only one parameter changes at a time, either the melting point or the enthalpy of fusion, see Table 1. For

the systems with a variance of two (water + additive), the melting point is actually not unique. The values reported here-under are the mean values of the fusion temperature in the conditions retained.

Their viscosity of course depends on the solid volume fraction $\phi = X \cdot \rho_s / \rho_{cr}$ and on the viscosity of the liquid phase, like for the ice slurry [22]:

Table 1. List of slurries considered in this study and some of their thermophysical properties

Code	Nature of the crystal particles	Additive in solution (mass fraction)	Gas pressure (MPa)	Melting point (°C)	Enthalpy of fusion (kJ/kg)
WG008	Ice	Mono-propylene-glycol (0.080)	-	-3	333.6
WG000	Ice	-	-	0	333.6
CO120	CO_2 hydrate	-	1.20	0	374.0
CO303	CO_2 hydrate	-	3.03	7.2	374.0
TB020	TBPB hydrate	TBPB (0.200)	-	7.2	204.0
Mx100	Mixed hydrate TBPB+ CO_2	TBPB (0.161)	0.1	7.2	220.0
Ma720	Mixed TBPB+ CO_2 hydrate	TBPB (0.200)	0.72	12.1	223.6

$$\mu_s = \mu_{ls}(x, T_m) \cdot \left(1 + 2.5 \cdot \phi + 10.05 \cdot \phi^2 + 273 \cdot 10^{-6} \cdot e^{16.6 \cdot \phi}\right) \tag{15}$$

Hydrate slurries are pseudoplastic fluids, well described by the Herschel-Bulkley's model respectively for the CO_2 hydrate (16) [33] and the TBPB or CO_2+TBPB hydrates (17) [34]:

$$\mu_s = 18 \cdot 10^{-4} \cdot e^{17.98 \cdot \phi} \cdot \dot{\gamma}^{n-1} \tag{16}$$

$$\mu_s = (0.273 + 2.15 \cdot \phi)^{4.65} \cdot \dot{\gamma}^{n-1} \tag{17}$$

3.2. Favoured flow conditions

When designing the secondary refrigeration system, once the slurry is chosen, two degrees of freedom are left: the tube diameter D of the SRL loop, and the mass fraction of crystals in the line 1-3, X_3. From the latter, resolution of (2)(3) yields the slurry mass flowrate. From this flow-rate and the diameter, the pressure drop ΔP_{tt} and the pumping power $\dot{W}_P$ are deduced as described in section 2.2.2. It must be noticed that only the linear sections of the SRL loop have been considered when deriving ΔP_{tt} and $\dot{W}_P$. In a real secondary refrigeration system, there are many other flow resistances that will multiply the values given herein by some units. This must be kept in mind when limits are specified for those two quantities.

The *favoured* flow conditions result from a trade-off between the intensity of turbulence in the line 1-3 (represented by the Reynolds number), the pumping power and the total pressure drop in the loop. With respect to energy efficiency only, large diameters and low slurry velocities are preferred because they reduce the pumping power. For extracting 30kW from the conditioned volume, one can expect the mechanical power of the compressor Cr to lie around 10kW. It will be considered herein that $\dot{W}_P$ remains a really auxiliary energy consumption if it lies around 100W (especially after the comment above about ΔP_{tt} and $\dot{W}_P$). However, the SRL loop must also be protected from *blocking*. Deposition of crystal particles would be avoided when the slurry velocity lies above 0.5-1m/s (ref.) and when the

flow is weakly turbulent (*Re*>3500-4000). This second concern comes in contradiction with the former one. Pressure is the third concern. The lowest pressure along the SRL loop, P_1 just upstream the circulation pump, depends on the crystallization process, especially when gaseous CO_2 is involved; in any case it is not less than atmospheric pressure. Just downstream the pump, pressure is maximal, $P_2 = P_1+\Delta P_{tt}$; the next requirement is that P_2 should be as low as possible. It is also considered that the pressure drop ΔP_{tt} should not lie far above one bar, under if possible.

Figure 2 presents how the Reynolds number, the pumping power $\dot{W}_P$ and the total pressure drop ΔP_{tt}

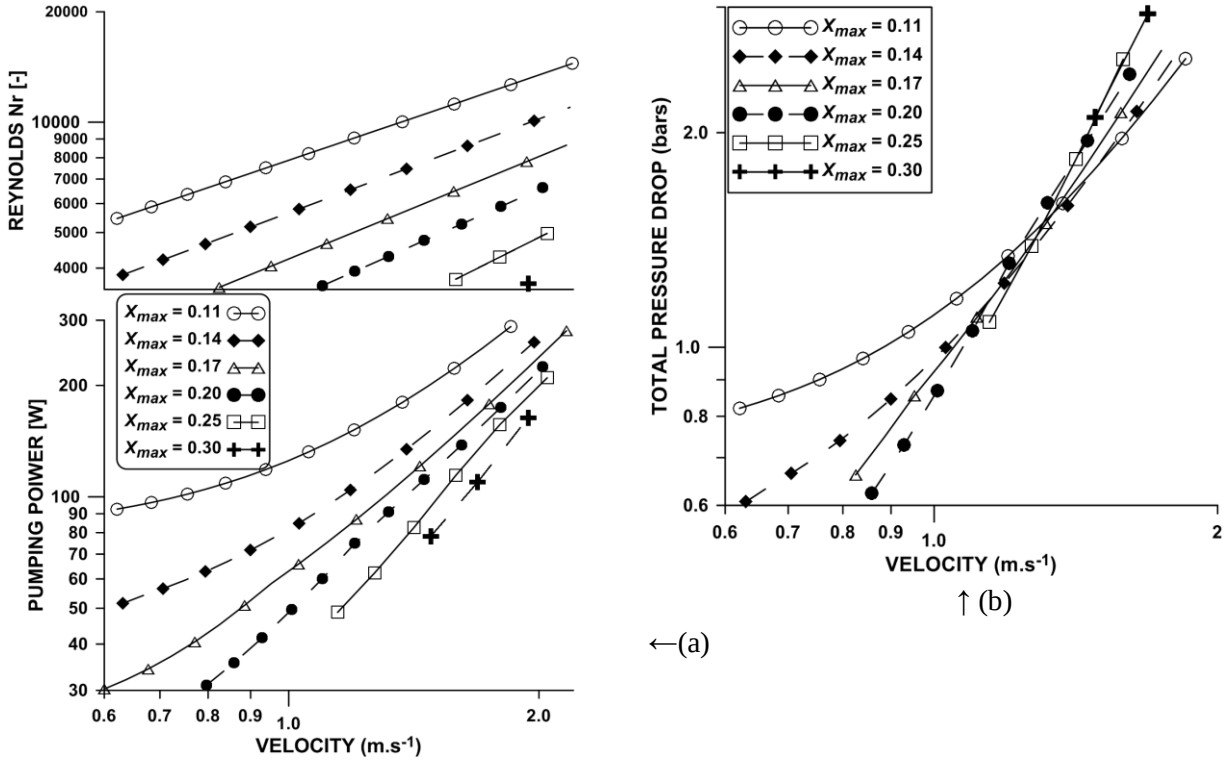

Fig. 2. CO_2 hydrate in water (slurry CO120): Reynolds number, pumping power (a) and total pressure drop (b) as functions of the slurry velocity in the SRL loop and of the mass fraction X_3.

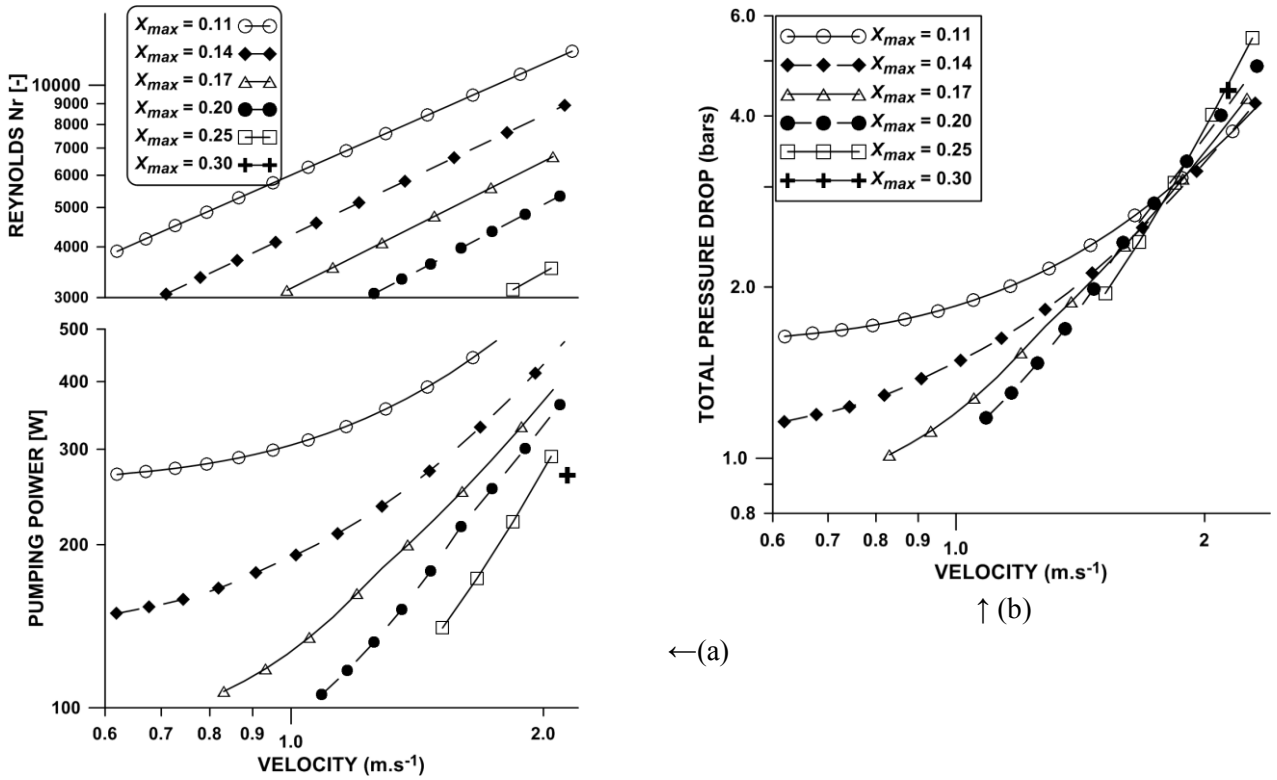

Fig. 3. Same as Fig. 2 but for mixed hydrate CO_2+TBPB in TBPB solution at 20% (slurry Ma720).

depend on both the slurry velocity u and the mass fraction X_3 (alias X_{max}) for the slurry of CO_2 hydrate in pure water at 0°C (code CO120). It can be seen that with the largest value of X_3 considered herein (0.30), the flow is turbulent only if u lies around 2m/s, which results in a pumping power slightly above the limit given above (150W), and a significantly too high pressure drop (3bars). This is due to the combination of a limited flow-rate, small diameters, and a large viscosity. On the opposite, the smallest value of X_3 investigated (0.11) leads to large Reynolds numbers, even at low velocities, but also pressure drops and pumping power that are not minimal. Also the combination of large flow-rates and weak viscosity is not optimal. Results for the other slurries are qualitatively similar, even if the slurry of mixed hydrate CO_2+TBPB in TBPB solution (see Fig. 3) makes the pressure drop and pumping power larger than in Fig. 2, because of 1) larger flow-rates due to a lower fusion enthalpy than for the CO_2 hydrate (see Table 1), and 2) a more viscous solution than pure water.

The other slurries yield similar results. It thus can be qualitatively inferred that intermediate values of X_3 meet the best the favoured flow conditions, especially with respect to pressure drop, see Fig. 2(b) and Fig. 3(b). This conclusion was unexpected. It is indeed often argued that two-phase fluids are beneficial to secondary refrigeration because they exchange their fusion enthalpy over a limited temperature glide. The present analysis supports the statement, but only to a certain extent. If slurries with too low a crystal mass fraction suffer from significant slurry flowrates that make pressure drops high, slurries with too high crystal mass fractions suffer from limited flow-rates and strong viscosity that make the flow laminar and increase the risk of particle deposition. To the authors' knowledge, optimization of secondary refrigeration systems as a trade-off between flow-rate and viscosity has never been mentioned before in the literature.

3.3. Global analysis: comparison of various slurries

The flow conditions of each of the seven slurries investigated herein are optimized as described in the previous section, so that their performance can be correctly compared. Results are reported in Fig. 4. About the flow conditions, it can first be seen that the design diameter (symbol ◁ in Fig. 4(a)) lies around 25-26mm for the slurries with water as solution (or with only 8% mono-propylene-glycol),

when it lies around 30-33mm for the slurries with the TBPB solution (16-20% in mass). The difference can mainly be related to the fusion enthalpy of the crystals: as it is weaker for the latter slurries, the flowrates and tube diameters must be larger. About performance, it clearly appears that the total power consumption (practically the compression energy of the AC cycle, symbol ▶) is

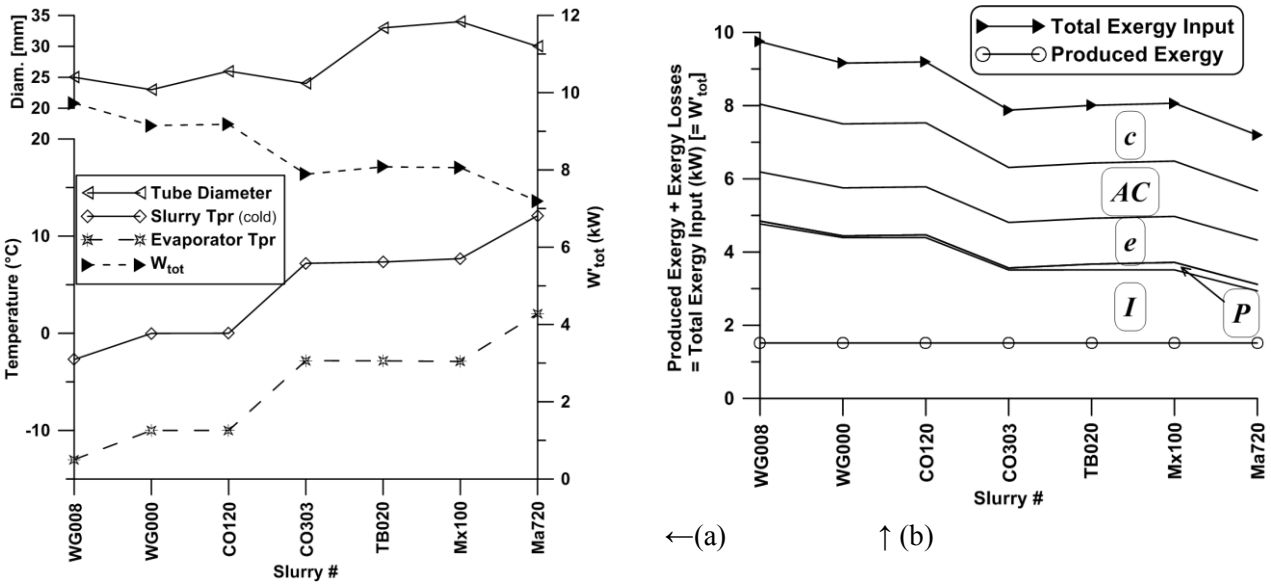

Fig. 4. Energetic (a) and exergetic (b) analyses of the secondary refrigeration process, once the flow conditions optimised independently for each slurry.

completely related to the crystal melting point (symbol ♢). Indeed the evaporation temperature of the AC cycle (symbol ❋) is always 10K less than the melting point because of the fixed thermal resistance at HXe. As a consequence; substituting the mixed hydrate CO_2+TBPB to classical ice slurry reduces the consumption of mechanical power by 25% approximately, and thus increases the global COP of the system from 3.1 (30/9.7) to 4.2 (30/7.2). Those figures should not be compared to direct expansion systems, which obviously have better performance but do not fulfil any limitation in the refrigerant volume.

The exergy analysis is presented in dimensional terms, so that the amount of produced exergy is the same for all the cases (consistently with the condition of a prescribed heat extraction $\dot{Q}_I$ at a prescribed temperature T_I) while the exergy input (equal to the sum of the produced exergy plus all the exergy losses) changes from case to case. Fig. 4(b) presents this exergy balance and it can be seen that the exergy input data indeed duplicate those of total power consumption in Fig. 4(a).

First, it can be mentioned that the exergy loss $\Delta\dot{B}_{Cg}$ cannot be seen in Fig. 4(b) (it actually lies between P and e) because the power consumption for CO_2 recompression, $\dot{W}_{Cg}$, is herein negligible.

The analysis can now highlight the main factor that affects performance efficiency of secondary refrigeration as a process: the entropic mean melting temperature of the slurry T_m. Energy and exergy analyses give complementary viewpoints on the changes from the slurry with ice (WG008) to that with mixed hydrate CO_2+TBPB (Ma720). First of all, the increase of T_m from -3 to 12°C significantly reduces the exergy loss in the HXI heat-exchanger $\Delta\dot{B}_I$ (-53%, the temperature difference $T_I - T_m$ changes by the same ratio). As a consequence, the evaporation temperature of the AC cycle, T_e, also increases by 15K (the exchanged flux and the thermal resistance of the HXe heat-exchanger are practically unchanged), while the condensation temperature, T_c, hardly changes (from 54 to 53.3°C). As a consequence, the COP of the endoreversible cycle operated between T_e and T_c is significantly improved (+38%), and the effective COP of the AC cycle as well (a prescribed isentropic compression

efficiency makes both quantities proportional, see (8)). This performance improvement has a twofold consequence: the power consumption $\dot{W}_{Cr}$, which is by far the main part of $\dot{W}_{tt}$, decreases significantly (-27%) while the exergy loss $\Delta\dot{B}_{AC}$ decreases by the same ratio, thus complementing the decrease of $\Delta\dot{B}_I$ for explaining the final result. The other exergy losses change by too low amounts for influencing noticeably the global performance.

Another point deserves being mentioned: the exergy analysis emphasizes the transition from (almost) purely aqueous solutions (slurries from WG008 to CO303) to solutions containing a large amount of TBPB (slurries from TB020 to Ma720), via the changes of the exergy loss $\Delta\dot{B}_P$ and of the pumping power $\dot{W}_P$.

4. Conclusion

Secondary refrigeration processes can be analysed in terms of energy and of exergy. The analysis shows that the most important feature with respect to energetic efficiency is the melting temperature of the crystals. This quantity mainly affects the COP of the refrigeration cycle (1st law) and the exergy loss due to heat transfer from the conditioned volume to the slurry (2nd law). The next important parameters are the fusion enthalpy and the slurry viscosity.

It has also been shown that the trade-off between prevention of particle deposition and reduction of pumping power / pressure drop leads to optimal flow conditions where the mass fraction of crystals in the slurry is neither too low nor too high. If latent heat is indeed more efficient than sensible heat, slurries are efficiently used when they contain an intermediate fraction of crystals (15-20%).

Acknowledgments

This study was mainly financed by the CNRS, via the *PEPS Energie* project *Formhydable*. It is now partly supported by the ANR project *CRISALHYD* (No ANR-14-CE05-0045). The authors also thank Camille de Romémont for her significant contribution to the numerical code.

Nomenclature

B, b	exergy, *J*
COP	Coefficient Of Performance
D	diameter of the channel, *m*
ΔH	enthalpy of crystallization, *J/kg*
L	half length of the loop, *m*
$\dot{m}$	mass flow rate, *kg/s*
P	pressure, *Pa*
R	thermal resistance, *K/kW*
$\dot{Q}$	heat flux, *W*
T	Entropic mean temperature, *K*
u	velocity, *m/s*
$\dot{W}$	mechanical power, *W*
x	solute mass fraction in the solution
X	solid mass fraction of crystals in the slurry
Y	mass fraction of water or gas in the crystal molecule

Greek symbols

η_{Bi}	internal exergetic efficiency of the Air Conditioning cycle, -
$\dot{\gamma}$	shear rate, s^{-1}
μ	dynamic viscosity, *kg/(m.s)*
ϕ	solid volume fraction of crystals in the slurry

Subscripts

1-8 positions shown in Fig. 1
c condensation
cr crystal
C compressor
e evaporator
E exterior
0 initial
g gas
I interior
ls liquid solution
m melting
P pump
r refrigerant
s slurry
tt total
w water

References

[1] Bellas I., Tassou S.A., Present and future applications of ice slurries. Int J Refrig 2005;28(1):115-21.

[2] Zhang P., Ma Z.W., An overview of fundamental studies and applications of phase change material slurries to secondary loop refrigeration and air conditioning systems. Renew Sust Energ Rev 2012;16(7):5021-58.

[3] Bel O., Lallemand A., Study of a two phase secondary refrigerant 1: Intrinsic thermophysical properties of an ice slurry. Int J Refrig 1999;22(3):164-74.

[4] Cezac P., Castaing-Lavignottes J., Reneaume J.M., Maunoury A., Description of ice slurry composition and enthalpy calculation from GE models: application to water-ethanol systems. Chem Eng Commun 2009;196(6):715-28.

[5] Fujii K., Yamada M., Enhancement of melting heat transfer of ice slurries by an injection flow in a rectangular cross sectional horizontal duct. Applied Thermal Eng 2013;60(1-2):72-78.

[6] Davies T.W., Slurry ice as a heat transfer fluid with a large number of application domains. Int J Refrig 2005;28(1):108-14.

[7] Guilpart J., Stamatiou E., Fournaison L., The control of ice slurry systems: an overview. Int J Refrig 2005;28(1):98-107.

[8] Compingt A., Blanc P., Quidort A., Slurry for refrigeration industrial kitchen application. in: Kauffeld M. (ed.) 8th IIR Conference on Phase Change Materials and Slurries for Refrigeration and Air Conditioning, Int Inst Refrigerat, Karlsruhe, Germany, 2009, pp. 135-44.

[9] Burgass R., Chapoy A., Duchet-Suchaux P., Tohidi B., Experimental water content measurements of carbon dioxide in equilibrium with hydrates at (223.15 to 263.15) K and (1.0 to 10.0) MPa. J Chem Thermodyn 2014;69:1-5.

[10] Eslamimanesh A., Mohammadi A.H., Richon D., Thermodynamic model for predicting phase equilibria of simple clathrate hydrates of refrigerants. Chemical Engineering Science 2011;66(21):5439-45.

[11] Loh J., Brodie G., Naim F., The roles of adsorption in hydrate precipitation. In: Johnson J.A. (ed.) Light Metals 2010. 2010. pp. 215-20.

[12] Darbouret M., Cournil M., Herri J.M., Rheological study of TBAB hydrate slurries as secondary two-phase refrigerants. Int J Refrig 2005;28(5):663-71.

[13] Lv X.F., Shi B.H., Wang Y., Gong J., Study on Gas Hydrate Formation and Hydrate Slurry Flow in a Multiphase Transportation System. Energy & Fuels 2013;27(12):7294-302.

[14] Ambuehl D., Madden M.E., CO2 hydrate formation and dissociation rates: Application to Mars. Icarus 2014;234:45-52.

[15] Golombok M., Ineke E., Luzardo J.C.R., He Y.Y., Zitha P., Resolving CO2 and methane hydrate formation kinetics. Environ Chem Lett 2009;7(4):325-30.

[16] Delavar H., Haghtalab A., Prediction of hydrate formation conditions using G(E)-EOS and UNIQUAC models for pure and mixed-gas systems. Fluid Phase Equilib 2014;369:1-12.

[17] Hsieh M.K., Ting W.Y., Chen Y.P., Chen P.C., Lin S.T., Chen L.J., Explicit pressure dependence of the Langmuir adsorption constant in the van der Waals-Platteeuw model for the equilibrium conditions of clathrate hydrates. Fluid Phase Equilib 2012;325:80-89.

[18] Chatti I., Delahaye A., Fournaison L., Petitet J.P., Benefits and drawbacks of clathrate hydrates: a review of their areas of interest. Energy Conv Manag 2005;46(9-10):1333-43.

[19] Li G., Hwang Y.H., Radermacher R., Review of cold storage materials for air conditioning application. Int J Refrig 2012;35(8):2053-77.

[20] Mayoufi N., Dalmazzone D., Delahaye A., Clain P., Fournaison L., Fuerst W., Experimental Data on Phase Behavior of Simple Tetrabutylphosphonium Bromide (TBPB) and Mixed CO2 + TBPB Semiclathrate Hydrates. Journal of Chemical and Engineering Data 2011;56(6):2987-93.

[21] El Abbassi I., Castaing-Lasvignottes J., Bedecarrats J.P., Dumas J.P., Mimet A., Energetic performances of a refrigerating loop using ice slurry. Applied Thermal Eng 2010;30(8-9):962-69.

[22] Guilpart J., Stamatiou E., Delahaye A., Fournaison L., Comparison of the performance of different ice slurry types depending on the application temperature. Int J Refrig 2006;29(5):781-88.

[23] Leiper A.N., Ash D.G., Mcbryde D.J., Quarini G.L., Improving the thermal efficiency of ice slurry production through comminution. Int J Refrig 2012;35(7):1931-39.

[24] Macphee D., Dincer I., Performance assessment of some ice TES systems. Int J Therm Sci 2009;48(12):2288-99.

[25] Meewisse J.W., Ferreira C.a.I., Ice slurries or brines in cold distribution systems? in: Hirs G.G. (ed.) ECOS 2000: From Thermo-Economics to Sustainability, Pts 1-4, Twente Enschede, Netherlands, 2000, pp. 857-68.

[26] Bi Y.H., Chen L.G., Sun F.R., Thermodynamic optimization for crystallization process of gas hydrate. Int J Energy Res 2012;36(2):269-76.

[27] Douzet J., Kwaterski M., Lallemand A., Chauuy F., Flick D., Herri J.M., Prototyping of a real size air-conditioning system using a tetra-n-butylammonium bromide semiclathrate hydrate slurry as secondary two-phase refrigerant - Experimental investigations and modelling. Int J Refrig 2013;36(6):1616-31.

[28] Ogawa T., Ito T., Watanabe K., Tahara K.I., Hiraoka R., Ochiai J.I., Ohmura R., Mori Y.H., Development of a novel hydrate-based refrigeration system: A preliminary overview. Applied Thermal Eng 2006;26(17-18):2157-67.

[29] Leiper A.N., Hammond E.C., Ash D.G., Mcbryde D.J., Quarini G.L., Energy conservation in ice slurry applications. Applied Thermal Eng 2013;51(1-2):1255-62.

[30] Bi Y.H., Guo T.W., Zhang L., Chen L.G., Sun F.R., Entropy generation minimization for charging and discharging processes in a gas-hydrate cool storage system. Applied Energy 2010;87(4):1149-57.

[31] Bouzid N., Saouli S., Aiboud-Saouli S., Entropy generation in ice slurry pipe flow. Int J Refrig 2008;31(8):1453-57.

[32] Pons M., Analysis of the adsorption cycles with thermal regeneration based on the entropic mean temperatures. Applied Thermal Eng 1997;17(7):615-27.

[33] Jerbi S., Delahaye A., Oignet J., Fournaison L., Haberschill P., Rheological properties of CO2 hydrate slurry produced in a stirred tank reactor and a secondary refrigeration loop. Int J Refrig 2013;36(4):1294-301.

[34] Clain P., Delahaye A., Fournaison L., Mayoufi N., Dalmazzone D., Furst W., Rheological Properties of tetra-n-butylphosphonium bromide hydrate slurry flow. Chemical Engineering Journal 2012;193:112-22.